

Short communication

# Influence of Cu content on ageing behavior of AlSiMgCu cast alloys

Guiqing Wang \*, Qingzhou Sun, Liming Feng, Luo Hui, Cainian Jing

Department of Material Science and Technology, Shandong Architectural Engineering Institute, Fengming Road, Lingang development District, Jinan 250101, PR China

Received 23 May 2005; accepted 18 November 2005

Available online 18 January 2006

## Abstract

The influence of Cu content on ageing behavior of Al–8Si–0.4Mg–*x*Cu alloys has been investigated by hardness measurement, differential scanning calorimetry (DSC) and transmission electron microscopy (TEM) analysis. Experiments have been conducted for Al–8Si–0.4Mg–*x*Cu alloys with 1 wt%Cu, 2 wt%Cu, 3 wt%Cu, and 4 wt%Cu produced in permanent moulds. Hardness has been estimated for ageing times varying from 1 h to 100 h. The results indicate that the maximum hardness increases clearly with the increase of Cu content, but the total increase in hardness during ageing ( $\Delta HV_{\max}$ ) decreases with addition of 1 wt%Cu and has a little increase with Cu content from 1 wt% to 4 wt%. Addition of Cu decreases the age hardening rate. The differential scanning calorimetry measurement and transmission electron microscopy analysis results suggest that addition of Cu to Al–8Si–0.4Mg alloy restrained the precipitation of  $\beta''$  and  $\beta'$  phases, but  $Q''$  phase precipitated for Al–8Si–0.4Mg–1Cu alloy, and  $Q''$  and  $\theta'$  phases precipitated for Al–8Si–0.4Mg–*x*Cu alloys with more than 1 wt%Cu. The precipitation behaviors and effect of precipitates on age hardening behaviors have been discussed. © 2005 Elsevier Ltd. All rights reserved.

## 1. Introduction

Aluminum–silicon (Al–Si) alloys, especially Al–Si hypoeutectic and eutectic alloys (containing 6–12% Si), are widely used in the automotive industry due to their excellent foundry characteristics and high mechanical properties. In order to improve the mechanical properties and machinability of Al–Si alloys, “modification” of the eutectic structure is usually carried out, where with the addition of a modifying agent such as Sr, Na or Sb, the morphology of the Si particles is transformed from coarse and acicular plates to a fine and fibrous form [1–3]. Addition of Mg and Cu to Al–Si alloys increases strength and reduces ductility [4,5]. For Al–Si–Mg and Al–Si–Cu–Mg alloys, a heat treatment consisting of solution treatment, quenching and ageing is often used to increase the strength by precipitating nanometer particles, which provide excellent obstacles for the dislocation movement [6,7]. For Al–Si–Mg alloys, the age hardening is caused by the precipitation of  $\beta''$  and/or  $\beta'$  phases (precursor of  $Mg_2Si$  phases) [8,9]. For Al–Si–

Mg–Cu alloys, the precipitation behaviors are rather complicated and several phases such as  $\beta$  ( $Mg_2Si$ ),  $\theta$  ( $CuAl_2$ ),  $S$  ( $CuMgAl_2$ ) or  $Q$  ( $Cu_2Mg_8Si_6Al_5$ ) in metastable situations may exist [10–12].

The present work focuses on how the changes in the amount of Cu affect the age hardening and precipitation behavior of Al–8Si–0.4Mg–*x*Cu cast alloys. Differential scanning calorimetry (DSC) measurement is used to estimate the precipitation behavior. Transmission electron microscopy (TEM) and energy dispersive spectrum (EDS) analysis are used to identify the precipitates.

## 2. Experimental details

All the alloys studied contain  $8 \pm 0.5\%$ Si,  $0.40 \pm 0.02\%$ Mg, together with additions of 1 wt%Cu, 2 wt%Cu, 3 wt%Cu, and 4 wt%Cu that were cast in permanent mould. Solution treatment was carried out in an electric furnace with a temperature control of  $\pm 3^\circ C$  for 24 h at  $500^\circ C$ , then quenched in water.

The quenched samples were aged at  $160^\circ C$  for times varying from 1 h to 100 h for hardness measurement. Hardness testing was carried out using a macro Vickers

\* Corresponding author. Tel.: +86 531 8392197.  
E-mail address: [fchang@sdu.edu.cn](mailto:fchang@sdu.edu.cn) (G. Wang).

hardness tester with a load of 20 kg and a dwell time of 30 s. Hardness test samples were lightly polished. Each Vickers hardness value was the average of at least five measurements.

Differential scanning calorimeter (DSC) determinations were performed in a NETZSCH DSC 404 instrument using a heating rate of  $10\text{ }^{\circ}\text{C min}^{-1}$ .  $1\text{--}2\text{ cm}^2$  were punched from quenched bars, then these were ground, using SiC paper (600 grade) to a thickness about 0.8 mm for DSC measurement. The DSC experiment was started about 0.5 h after solution treatment. During DSC measurements, samples were protected under an argon atmosphere with a flow rate of  $80\text{ ml min}^{-1}$ ; a super purity aluminum specimen of equal mass was used as a reference.

In a DSC experiment, the rate of heat evolution (or absorption) is plotted as a function of temperature, and a precipitation event is manifested as an exothermic peak. For a given heating rate, the peak temperature depends upon the specific precipitation process.

TEM specimens were thinned by mechanical polishing, followed by ion milling. They were then examined in a H-800 TEM transmission electron microscope operating at 150 kV. The precipitates were identified by selected area electron diffraction and energy dispersive spectrum (EDS).

### 3. Results and analyses

#### 3.1. Age hardening characteristics

Plots of hardness against time during ageing at  $160\text{ }^{\circ}\text{C}$  for quenched samples of Al-8Si-0.4Mg- $x$ Cu alloys with 0 wt%Cu, 1 wt%Cu, 2 wt%Cu, 3 wt%Cu, and 4 wt%Cu are plotted in Fig. 1. Subtracting the hardness in as quenched conditions from the maximum hardness gives the total increase in hardness  $\Delta\text{HV}_{\text{max}}$  during ageing just as shown in Table 1, which shows the age hardening ability of alloys.

Hardness in both of the as quenched conditions and peak-aged conditions increases strongly with increase of

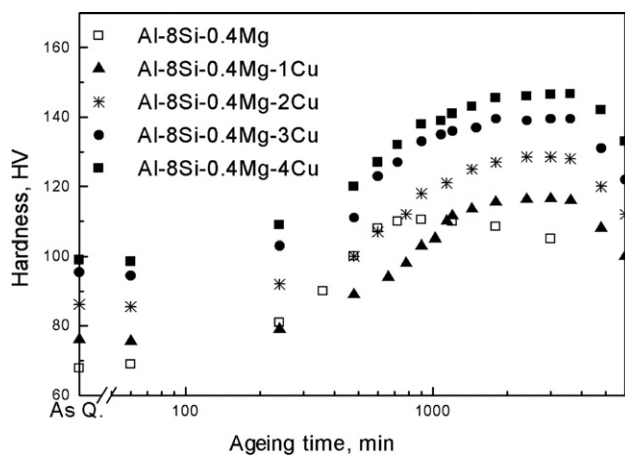


Fig. 1. Vickers hardness as a function of ageing time during ageing at  $160\text{ }^{\circ}\text{C}$  for quenched samples.

Table 1  
Vickers hardness and  $\Delta\text{HV}_{\text{max}}$  for Al-8Si-0.4Mg- $x$ Cu alloys

Alloy	Hardness (HV)		$\Delta\text{HV}_{\text{max}}$
	As quenched	Peak aged	
Al-8Si-0.4Mg	68.8	111	42.2
Al-8Si-0.4Mg-1Cu	77	116.5	39.5
Al-8Si-0.4Mg-2Cu	86.7	129	42.3
Al-8Si-0.4Mg-3Cu	95.4	140	44.6
Al-8Si-0.4Mg-4Cu	99	146.6	47.6

Cu content. The increase of hardness in as quenched conditions with increase of Cu content indicates that the solid-solution strengthening of Al-8Si-0.4Mg- $x$ Cu alloys is enhanced with increase of Cu content. For Cu-free Al-8Si-0.4Mg alloy, hardness begins to increase in a few minutes and maximum hardness is obtained for about 700 min, the total increase in hardness  $\Delta\text{HV}_{\text{max}}$  is about 42.2 HV. For Cu containing Al-8Si-0.4Mg- $x$ Cu alloys, precipitation does not begin for at least 60 min and maximum hardness is observed for about 3000 min. The total increase in hardness  $\Delta\text{HV}_{\text{max}}$  decreases from 42.2 HV to 39.5 HV with addition of 1 wt%Cu to Al-8Si-0.4Mg alloy and increase from 39.5 HV to 47.6 HV with addition of Cu from 1 wt% to 4 wt%. This indicates that addition of Cu to Al-8Si-0.4Mg alloy increases the age hardening ability slightly, moreover Cu addition decreases the age hardening rate. The strong increase of maximum hardness during ageing with increase of Cu content is mainly the results of solid-solution strengthening of Cu on  $\alpha$  (Al) matrix.

#### 3.2. Precipitation behaviors

DSC traces obtained by heating the as quenched specimens of the examined Al-8Si-0.4Mg- $x$ Cu alloys with 0 wt%Cu, 1 wt%Cu, 2 wt%Cu, 3 wt%Cu, and 4 wt%Cu are shown in Fig. 2 respectively.

Each DSC trace exhibited two exothermic peaks overlapped in the temperature range of  $180\text{--}340\text{ }^{\circ}\text{C}$ . Previous

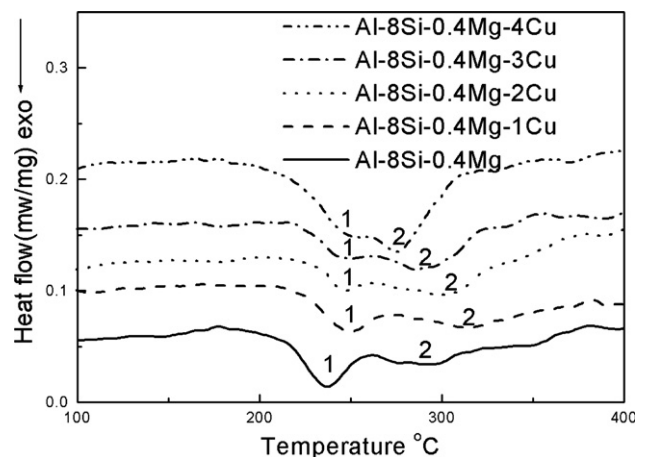


Fig. 2. DSC traces at a heating rate of  $10\text{ }^{\circ}\text{C min}^{-1}$  for as quenched samples.

DSC investigations on Al–Mg–Si–Cu wrought alloys [8,13–17] showed that exothermic peak 1 in the temperature range of 180–260 °C corresponded to the precipitation of coherent  $\beta''$  and/or  $\theta''$ ,  $S''$ ,  $Q''$  phases, and exothermic peak 2 in the temperature range of 260–340 °C was caused by the precipitation of semi-coherent  $\beta'$  and/or  $\theta'$ ,  $S'$ ,  $Q'$  phases. For Al–8Si–0.4Mg alloy, peaks 1 and 2 should be related to the precipitation of  $\beta''$  and  $\beta'$  phases [13]. For Cu containing Al–8Si–0.4Mg– $x$ Cu alloys, several precipitates would form, which will be identified by TEM analyses in the following.

The position of exothermic peak on DSC curves is related to precipitation dynamics [18]. Fig. 2 shows that the temperature of peak 1 for Cu containing alloys was higher than that of Cu free alloys. This indicates that higher precipitation dynamic is needed in Cu containing alloys. This is consistent with the above hardness analysis result that Cu addition decreases the age hardening rate.

For Cu containing alloys, the position of peak 1 did not change, but peak 2 shifted to low temperature with increase of Cu content. Peaks 2 and 1 merged into one peak for 4 wt%Cu containing alloys. This suggests that precipitation of semi-coherent phases is promoted with increase of Cu content, and the semi-coherent and coherent phases would co-precipitate during ageing in higher Cu containing alloys, which will be testified by following TEM analyses.

Unlike wrought alloys, exothermic peak at around 100–200 °C corresponding to the precipitation of GP zones was not detected. Similar DSC traces for Al–Si–Mg cast alloys were also obtained by other researchers [12], which indicate that cast Al–Si–base alloys are quenching sensitive and GP zones have formed before heating.

Samples of Al–8Si–0.4Mg–1Cu and Al–8Si–0.4Mg–3Cu alloys aged at 160 °C for 30 h with peak hardness and 100 h in over aged condition were examined using TEM analysis as shown in Fig. 3 to 4 respectively.

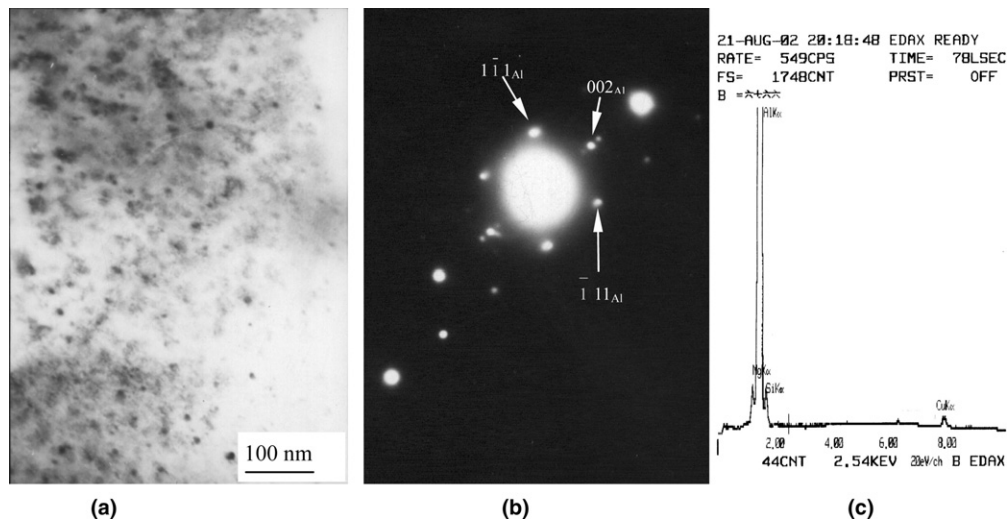


Fig. 3. TEM micrograph for Al–8Si–0.4Mg–1Cu alloy aged at 160 °C for 30 h (a), the correspondent SADP (b) and EDS (c) for dot shaped phases.

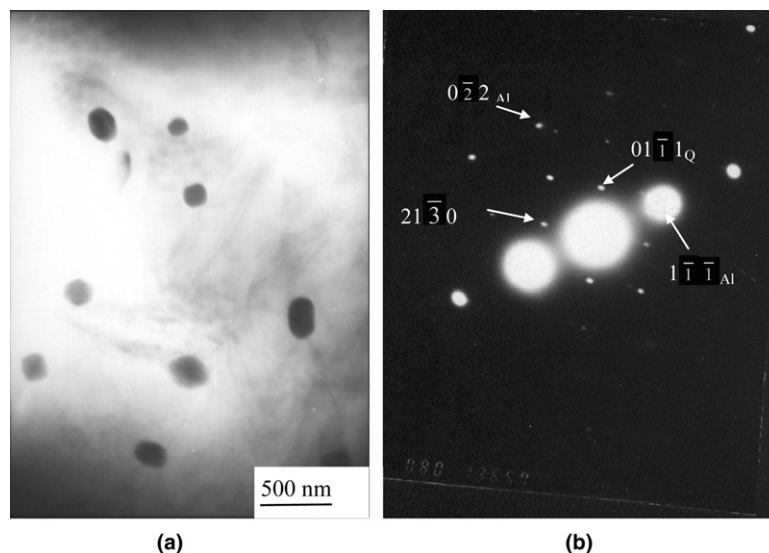


Fig. 4. TEM micrograph for Al–8Si–0.4Mg–1Cu alloy aged at 160 °C for 100 h (a) and SADP (b).

For Al–8Si–0.4Mg–1Cu alloy, ageing at 160 °C for 30 h produces dot shaped phases as shown in Fig. 3, that were confirmed as quaternary  $Q''$  phases (precursor of  $Q$ ) by the selected area diffraction pattern (SADP) and energy dispersive spectrum (EDS). Ageing for 100 h at 160 °C produces complete transition to big spheroids, as can be seen from Fig. 4, which were confirmed as hexagonal  $Q$  phase with  $a = 1.036$  nm and  $c = 0.404$  nm by the select area diffraction pattern (SADP).

For Al–8Si–0.4Mg–3Cu alloy ageing at 160 °C for 30 h, rod shaped phases formed on dislocations were observed except for dot shaped  $Q''$  phases, as shown in Fig. 5, which were confirmed as  $\theta'$  phases by the selected area diffraction pattern (SADP) and energy dispersive

spectrum (EDS) analyses. Ageing for 100 h at 160 °C produces rectangle plates in addition to spheroids for  $Q$  phases, as can be seen from Fig. 6. The rectangle plates were confirmed as  $\theta$  phase with  $a = 0.6066$  nm and  $c = 0.4847$  nm by the select area diffraction pattern (SADP).

#### 4. Discussions

For Al–8Si–0.4Mg alloy, age hardening is caused by the precipitation of needle shaped  $\beta''$  and/or  $\beta'$  phases [13]. Addition of 1 wt%Cu to this alloy,  $Q''$  phases precipitate instead of  $\beta''$  and/or  $\beta'$  phases, which indicates that the combining energy of Mg with Al, Cu and Si is stronger

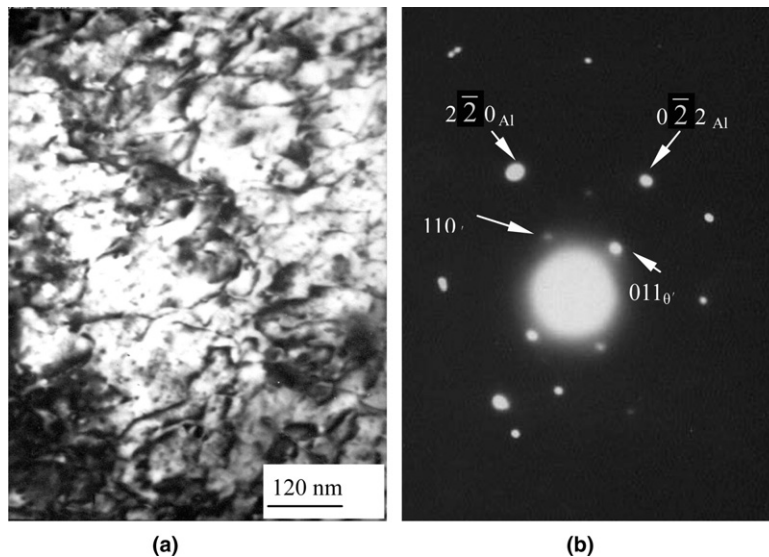


Fig. 5. TEM micrograph for Al–8Si–0.4Mg–3Cu alloy aged at 160 °C for 30 h (a) and the correspondent SADP for rod shaped phases (b).

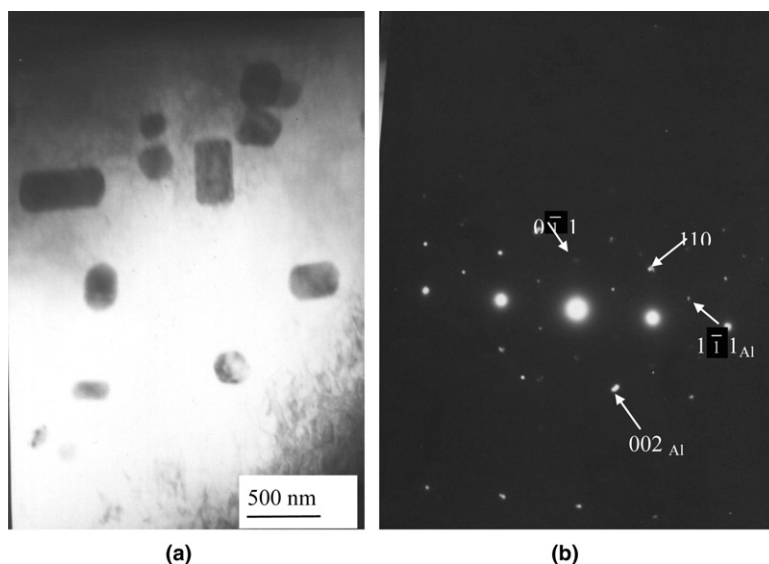


Fig. 6. TEM micrograph for Al–8Si–0.4Mg–3Cu alloy aged at 160 °C for 100 h (a) and the correspondent SADP for rectangle plates (b).

than that of Mg with Si. The precipitation of  $\theta'$  phases was promoted with increase of Cu content. The co-precipitation of  $Q''$  and  $\theta'$  phases in Al–8Si–0.4Mg–3Cu alloys suggests that Cu atoms solved in  $\alpha$  (Al) matrix combine with Mg, Si, Al to form  $Q''$  phase first and the remainder Cu atoms combine with Al to form  $\theta'$  phase on dislocations. The age hardening response depends on the volume fraction, shape and structure of precipitates formed during ageing. The decrease of the age hardening ability with addition of 1 wt%Cu to Al–8Si–0.4Mg alloy as shown in Fig. 1 and Table 1 indicates that the hardening ability of dot shaped  $Q''$  phases on  $\alpha$  (Al) matrix is less than that of needle shaped  $\beta''$  and/or  $\beta'$  phases. The  $\theta'$  precipitates forming on dislocations provide less obstacles for dislocation movement, which should be the cause of slow increase of  $\Delta HV_{\max}$  with increase of Cu content.

For Cu containing alloys, over-aged structures appear when ageing 100 h at 160 °C, but hardness value after ageing at 160 °C for 100 h remains higher than before ageing as shown in Fig. 1. This is related to the distribution of precipitates after over-ageing. Other than accumulated in grain boundaries, most of precipitates accumulated within  $\alpha$  (Al) after over-ageing as shown in Figs. 4(a) and 6(a), which only weakens the hardening ability of precipitates on  $\alpha$  (Al).

## 5. Conclusions

- (1) Addition of Cu to Al–8Si–0.4Mg alloy decreases the age hardening rate. With increase of Cu content, the solid-solution strengthening of Al–8Si–0.4Mg– $x$ Cu alloys is enhanced, but the age hardening ability increases slightly, moreover it decreases a little with addition of 1 wt%Cu. The strong increase of maximum hardness during ageing with increase of Cu content is mainly the results of solid-solution strengthening of Cu on  $\alpha$  (Al) matrix.
- (2) For Al–8Si–0.4Mg–1Cu alloy, age hardening precipitates were dot shaped  $Q''$  phases whose hardening ability on  $\alpha$  (Al) matrix is less than that of needle shaped  $\beta''$  and/or  $\beta'$  phases in Al–8Si–0.4Mg alloys. The precipitation of  $\theta'$  phases was promoted with increase of Cu content. For Al–8Si–0.4Mg–3Cu alloy, age hardening was caused by the co-precipitation of dot shaped  $Q''$  phases and wavelike  $\theta'$  phases. The precipitation of  $\theta'$  phases during ageing produces less increase in hardness because of forming on dislocations.

## Acknowledgments

We gratefully acknowledge the support of Shandong Science and Research Foundation for Encouraging Exemplary Middle and Young People (Grant No. 2004BS04014).

## References

- [1] Dudyk M, Ficek B, Suchanek B, Wasilewski P. The influence of modification, using strontium and antimony, on the properties of AlSi6Cu2Mg and AlSi8Cu4MgMn aluminium alloys used for automobile castings. *Cast Metals* 1990;3:158–62.
- [2] Dahle AK, Nogita K, Zindel JW, McDonald SD, Hogan LM. Eutectic nucleation and growth in hypoeutectic Al–Si alloys at different strontium levels. *Metall Mater Trans A* 2001;32A:949–60.
- [3] Caceres CH, Wang QG. Solidification conditions, heat treatment and tensile ductility of Al–7Si–0.4Mg casting alloys. *AFS Trans* 1996;104:1039–43.
- [4] Samuel FH, Samuel AM, Liu H. Effect of magnesium content on the ageing behaviour of water-chilled Al–Si–Cu–Mg–Fe–Mn(380) alloy castings. *J Mater Sci* 1995;30:2531–40.
- [5] Moustafa MA, Samuel FH, Doty HW, Valtierra S. Effect of Mg and Cu additions on the microstructural characteristics and tensile properties of Sr-modified Al–Si eutectic alloys. *Int J Cast Metals Res* 2002;14:235–53.
- [6] Cáceres CH. Microstructure design and heat treatment selection for casting alloys using the quality index. *J Mater Eng Perform* 2000;9:215–21.
- [7] Ouellet P, Samuel FH. Effect of Mg on the ageing behavior of Al–Si–Cu 319 type aluminum casting alloys. *J Mater Sci* 1999;34:4671–97.
- [8] Shivkumar S, Keller C, Apelian D. Ageing behavior in cast Al–Si–Mg alloys. *AFS Trans* 1990;98:905–11.
- [9] Kashyap KT, Murali S, Raman KS, Smurthy KS. Overview casting and heat treatment variables of Al–7Si–Mg alloy. *Mater Sci Technol* 1993;9:189–203.
- [10] Barlow IC, Rainforth WM, Jones H. The role of silicon in the formation of the (Al<sub>3</sub>Cu<sub>6</sub>Mg<sub>2</sub>)  $\sigma$  phase in Al–Cu–Mg alloys. *J Mater Sci* 2000;35:1413–81.
- [11] Reif W, Yu S, Dutkiewicz J, Ciach R, Król J. Pre-ageing of AlSiCuMg alloys in relation to structure and mechanical properties. *Mater Des* 1997;18:253–6.
- [12] Mishra RK, Smith GW, Baxter WJ, Sachdev AK, Franetovic V. The sequence of precipitation in 339 aluminum castings. *J Mater Sci* 2001;36:461–8.
- [13] Zhang DL, Zheng L. The quench sensitivity of cast Al–7Wt Pct Si–0.4 Wt Pct Mg alloy. *Metall Mater Trans A* 1996;27A:3983–91.
- [14] Crowell N, Shivkumar S. Solution treatment effects in cast Al–Si–Cu alloys. *AFS Trans* 1995;103:721–6.
- [15] Zhen L, Kang SB. DSC analysis of the precipitation behavior of two Al–Mg–Si alloys naturally aged for different times. *Mater Lett* 1998;37:349–53.
- [16] Edwards GA, Stiller K, Gunlop GL, Couper MJ. The precipitation sequence in Al–Mg–Si alloys. *Acta Mater* 1998;46:3893–904.
- [17] Kang HG, Kida M, Miyahara H, Ogi K. Age-hardening characteristics of Al–Si–Cu-base cast alloys. *AFS Trans* 1999;107:507–15.
- [18] Vijayalakshmi M, Seetharaman V, Raghunathan VS. Cellular decomposition in Al–Zn alloys. *Acta Mater* 1982;30:1147–56.